VII International Conference on Particle-Based Methods
PARTICLES 2021
P. Wriggers, M. Bischoff, E. Oñate, A. Düster & T. Zohdi (Eds)

SPH BASED STUDY OF CONFINED MICROFLOWS CHARACTERIZED BY ABRUPT CHANGES IN CROSS-SECTIONAL AREA

Efstathios Chatzoglou[1], Filippos Sofos[2] and Antonios Liakopoulos[1,*]
[1]Department of Civil Engineering, University of Thessaly, Pedion Areos, 38334 Volos, Greece
[*]e-mail: aliakop@uth.gr, web page: http://liakopoulos.users.uth.gr

[2] Physics Department, University of Thessaly, 35100, Lamia, Greece

Key words: Microflows, Confined flows, Laminar flow, SPH, LAMMPS, DualSPHysics

Abstract. *In this paper, we investigate the application of Smoothed Particle Hydrodynamics (SPH) method to the computation of flows in microchannels with sudden expansion. Numerical modeling with SPH involves the treatment of flowing matter as distinct mass points, leading to discretization of the Navier-Stokes equations (or other appropriate PDEs) and providing great flexibility to handle large deformations. The computational methodology exhibits similarities with other particle methods, such as Molecular Dynamics (MD), Dissipative Particle Dynamics (DPD), and Smooth Dissipative Particle Dynamics (SDPD). These similarities lead relatively easily to the development of a weakly compressible SPH within the framework of Large-scale Atomic/Molecular Massively Parallel Simulator (LAMMPS). The LAMMPS environment, albeit mostly intended to MD simulations near the atomic scale, provides a fully parallelized framework for particle simulations, such as SPH. In this work we studied microchannel flows of variable cross section. Sudden expansions generate strong discontinuities in the flow field. Flow models based on various inlet/outlet boundary conditions for example, Periodic/Fixed BCs, and their implementations are presented in the context of 3-D simulations. Minor artifacts may be observed near the wall corner discontinuities, but, overall, the SPH captures the main flow characteristics and achieves very good accuracy.*

1 INTRODUCTION

Fluid flow numerical simulation has gained wide acceptance in various branches of industry over the last decades. Conventional methods have faced insurmountable difficulties in some cases where the fluid flow involves geometrical complexities, chemical reactions, and scale problems, to mention a few [1,2]. Therefore, the use of novel numerical tools, which have been validated and proven reliable, may provide satisfying solutions in many industrial problems, such as chemical analysis, biomedicine, microscopic interactions, and phenomena which are usually neglected at the macroscopic scale [3].

Numerical methods are broadly classified into Lagrangian, Eulerian and mixed type Langragian-Eulerian methods. In the non-adaptive Eulerian approach, a fixed Cartesian mesh covers the computational domain; no remeshing is performed and large deformations of the continuum are resolved possibly without mesh adaptation. In adaptive Eulerian methods the

mesh adapts to the solution and allows the computation of rather challenging flow fields. However, adaptive Eulerian methods may have limitations in terms of cost and convergence to the correct solution. In the Lagrangian approach, the mesh (when used) moves naturally and follows the boundaries, leading to a simplified numerical handling of free surfaces and interfaces, since no grid points are needed outside the continuum. Yet, large deformation of the continuum may negatively affect the numerical accuracy [4]. To remedy this issue, various adaptive Lagragian methods have been proposed.

Smoothed Particle Hydrodynamics (SPH) is a mesh-free method, based on the concept of describing the flow by following the motion of fluid particles (point masses). All the information associated with the fluid particles is associated with each point mass, which interacts with other neighboring particles under common physical laws, based on a built-in approximation utilizing a kernel function [5,6]. A number of SPH formulations have been proposed covering the whole spectrum between the original Lagrangian formulation and recent Eulerian variants [7,8]. The SPH computational methodology exhibits similarities with other particle methods, such as Molecular Dynamics (MD), Dissipative Particle Dynamics (DPD), and Smooth Dissipative Particle Dynamics (SDPD). A brief discussion on the scales, where these methods are appropriate, is given in [9]. It should be noticed that SPH is a numerical approximation of the partial differencial equations of continum mechanics in contradistiction with MD, DPD, SDPD which are valid in flows where the continum theory may or may not break down [10-11].

The mesh-less nature of SPH and the kernel truncation close to boundaries can cause difficulties in enforcing solid boundary conditions [12]. Moreover, there is still considerable ambiguity in the simulation of highly turbulent flows without the demand of vast computational time, especially when the fluid passes through confined channels that demand special boundary treatment for accuracy very close to the solid walls.

In this work, we have investigated the SPH performance in simulating the flow inside 3D closed channels with the presence of an abrupt change in cross-section area. Emphasis has been given to the comparison of inlet/outlet boundary conditions. Simulations were run with the SPH method as implemented in LAMMPS [13,14]. The results show good accuracy in terms of comparison with the analytical solutions. However, further study is necessary in order to resolve convergence issues close to the fluid-wall interface and to improve the accurate imposition of boundary conditions.

2 MATHEMATICAL RELATIONS

SPH is a method in which the fluid is divided into a set of discrete moving particles. The governing equations describe the co-moving evolutions of ρ (density), r (position), u (velocity), e (energy per unit mass), and Q (heat flux-vector) [13]

$$\frac{d\rho}{dt} = -\rho\nabla \cdot u \tag{1}$$

$$\frac{du}{dt} = -\frac{1}{\rho}\nabla \cdot P + \nabla \cdot [\nu(\nabla u + \nabla u^T)] + g \tag{2}$$

$$\frac{de}{dt} = -\rho P : \nabla v - \frac{1}{\rho}\nabla Q \tag{3}$$

where P is the pressure, v the kinematic viscosity and g the external force (per unit mass). SPH interpolates the set of the above field variables by means of kernel interpolation. For a representative function $f(\boldsymbol{r})$, we write

$$f(\boldsymbol{r_i}) = \sum_j m_j \frac{f_j}{\rho_j} W(\boldsymbol{r}_i - \boldsymbol{r}_j) \tag{4}$$

where W is the kernel function. The sum in Eq. 4 theoretically extends over all the fluid particles, yet only particles for which $r_i - r_j < h$ need to be considered for appropriately selected kernel function of compact support. This saves computational cost but can lead to inaccuracies close to boundaries (especially wall-fluid interface).

2.1 Local Density approximation

Local density which is calculated for each particle, is a smoothed quantity obtained from the contribution of neighbor particles within the range of kernel smoothing length (h).

$$\rho_i = \sum_j m_j \frac{\rho_j}{\rho_j} W_{ij} \tag{5}$$

Here W is the kernel function and i, j two different particles.

2.2 SPH formulation of the Navier-Stokes equations

In the SPH models of our simulation we employ a weakly compressible form of governing equations which are written in a general form as

$$\frac{\mathrm{D}\rho_i}{\mathrm{Dt}} = \sum_{j=1}^{\mathrm{N}} \mathrm{m}_j \upsilon_{ij}^{\beta} \frac{\partial \mathrm{W}_{ij}}{\partial x_i^{\beta}} \tag{6}$$

$$\frac{\mathrm{D}\upsilon_i^a}{\mathrm{Dt}} = -\sum_{j=1}^{\mathrm{N}} \mathrm{m}_j \left(\frac{\sigma_i^{\alpha\beta}}{\rho_i^2} + \frac{\sigma_j^{\alpha\beta}}{\rho_j^2} \right) \frac{\partial \mathrm{W}_{ij}}{\partial x_i^{\beta}} + \mathrm{b}_i^a \tag{7}$$

$$\frac{\mathrm{De}_i}{\mathrm{Dt}} = \frac{1}{2} \sum_{j=1}^{\mathrm{N}} \mathrm{m}_j \left(\frac{\mathrm{p}_i}{\rho_i^2} + \frac{\mathrm{p}_j}{\rho_j^2} \right) \upsilon_{ij}^{\beta} \frac{\partial \mathrm{W}_{ij}}{\partial x_i^{\beta}} + \frac{\mu_i}{2\rho_i} \varepsilon_i^{a\beta} \varepsilon_i^{a\beta} \tag{8}$$

Here, $\upsilon_{ij} = \upsilon_i - \upsilon_j$, $\varepsilon^{\alpha\beta} = \frac{\partial \upsilon^{\beta}}{\partial x^{\alpha}} + \frac{\partial \upsilon^{\alpha}}{\partial x^{\beta}} - \frac{2}{3}(\nabla \cdot \mathbf{V})\delta^{\alpha\beta}$, $\sigma^{\alpha\beta} = -\mathrm{p}\delta^{\alpha\beta} + \tau^{\alpha\beta}$ and $\tau^{\alpha\beta}$ are the components of the stress deviator, W_{ij} the kernel (weight) function, m_j (mass), ρ_i (density), p_i (pressure), $(\upsilon^1, \upsilon^2, \upsilon^3)$ velocity, and μ_i the dynamic viscosity coefficient of the i^{th} particle.

The pressure field is computed through the Tait's equation of state

$$P = B\left[\left(\frac{\rho}{\rho_0} \right)^{\gamma} - 1 \right] \quad , \quad \text{where } B = \frac{c_0^2 \rho_0}{\gamma} \text{ and } \gamma = 7. \tag{9}$$

2.3 SPH treatment of viscosity

The equation of motion is derived after the evaluation of the gradient of the pressure tensor, suitable for implementation in particle methods, such as MD and SPH. Considering only inertia and pressure forces the interactions between neighboring particles are

$$\mathbf{f}_i = m_i \frac{\mathrm{d}\mathbf{v}_\mathbf{i}}{\mathrm{dt}} = -\sum_j m_i m_j \left(\frac{P_i}{\rho_i^2} + \frac{P_j}{\rho_j^2} \right) \nabla_j W_{ij} \tag{10}$$

The calculation is embedded in the SPH code, without any special consideration by the user. To incorporate viscosity, an additional viscous term Π_{ij} is introduced and the above expression for the pair-wise forces takes the form

$$\mathbf{f}_i = -\sum_j m_i m_j \left(\frac{P_i}{\rho_i^2} + \frac{P_j}{\rho_j^2} + \Pi_{ij} \right) \nabla_j W_{ij} \tag{11}$$

with

$$\Pi_{ij} = -ah \frac{c_i + c_j}{\rho_i + \rho_j} \frac{v_{ij} \cdot r_{ij}}{r_{ij}^2 + \varepsilon h^2} \tag{12}$$

Here *i*, *j* are particle indices, c is the speed of sound, α is an auxiliary factor for control of dissipation, and ε an auxiliary factor used to avoid singularities when $\mathbf{x}_{\mathrm{ij}} \to 0$. As a rule of thumb $\varepsilon \approx 0.01$. Artificial viscosity can be expressed in terms of an effective kinematic viscosity ν as: $\nu = ahc/8$ [13].

For laminar flow, an expression for derivatives is proposed [15] which seems to reproduce laminar flows correctly

$$f_i = -\sum_j m_i m_j \left(\frac{P_i}{\rho_i^2} + \frac{P_j}{\rho_j^2} \right) \nabla_j W_{ij} + \sum_j \frac{m_j (\mu_i + \mu_j) v_{ij}}{\rho_i \rho_j} \left(\frac{1}{r_{ij}} \frac{\partial W_{ij}}{\partial r_i} \right) \tag{13}$$

Both expressions (Eqs. 10 and 11) can be easily adopted in the LAMMPS code. Eq.(11) performs better in high Reynolds numbers [13] while Eq. (13) is well-suited for laminar flows [13]. Equation 13 is utilized in the present work.

3 THE SIMULATION MODEL

3.1 Three-dimensional flows in LAMMPS

Three-dimensional channels with constant cross-section and sudden expansion are investigated. In all cases fluid density is considered ρ=1000 kg/m^3 and constant, even if some small variations occurred. Simulation time step is set to Δt=0.5μs, in compliance with the CFL criterion for SPH simulations. The simulation time consists of 5×10^6 steps until equilibration, followed by another run of 5×10^6 steps in which particles attain random velocities, and, finally, a production run where an external force drives the flow until it becomes fully developed and reaches steady state. The driving force is F_{ext}=0.001 N/particle.

In order to compare the solution with analytical results, F_{ext} is utilized in order to compute pressure difference $N \cdot F_{ext} \leftrightarrow \Delta p \cdot A$, where A is the cross-section area.

Dynamic viscosity is set to μ=0.001 Pas, which corresponds to a kinematic viscosity of $\nu=10^{-6}$ m^2/s. More information on the model parameters and boundary conditions can be found on Table 1.

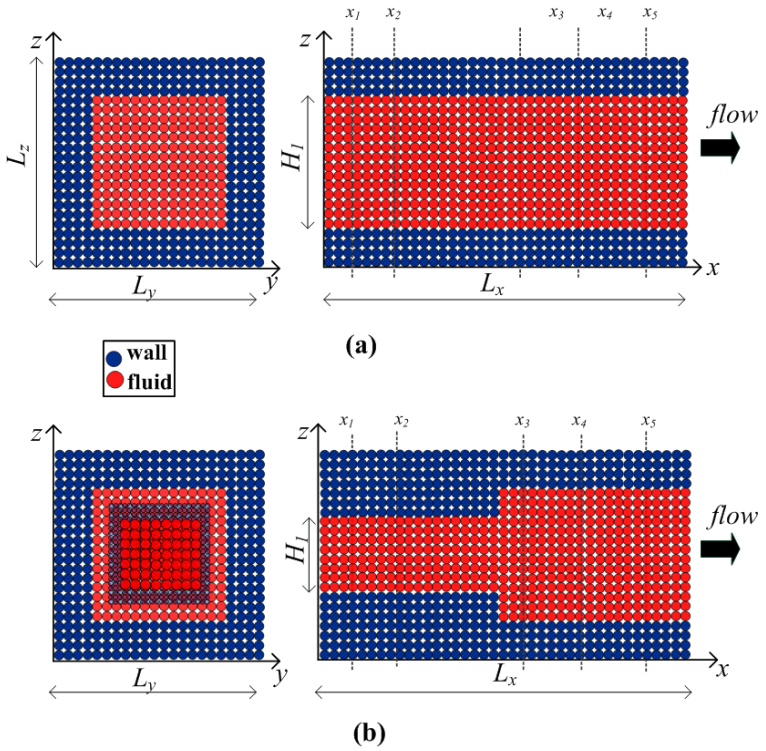

Figure 1. The 3D channel models a) constant cross-section, b) with sudden expansion

Table 1. Numerical parameters of 3D channel flows. *L* is the computational length in each direction (*x*, *y*, or *z*), BCs is the method of boundary conditions treatment at each direction, and N_p the number of particles.

Channel type	L_x(m) ($\times 10^{-4}$)	L_y(m) ($\times 10^{-4}$)	L_z(m) ($\times 10^{-4}$)	h(m) ($\times 10^{-4}$)	e_r (%)	BCs (xyz)	N_p
Constant Cross section	36.88	11.04	11.04	9.85	0	FFF	37178
Constant Cross section	36.88	11.04	11.04	9.85	0	PFF	37178
Sudden Expansion	18.44	11.04	11.04	4.925	100	FFF	10328
Sudden Expansion	18.44	11.04	11.04	4.925	100	PFF	10328

4 RESULTS AND DISCUSSION

4.1 Straight channel with square cross-section of constant area

A 3D channel with constant *H1*=0.985 mm (see figure 1) is investigated with two different BCs in the flow direction. At first, we consider a full channel in which the fluid transports from one side to the other (one moment of the flow) using FBCs. In order to evaluate the results, the same problem is also simulated under PBCs. Each particle being located outside the computational domain (downstream) is automatically inserted to the other side, having the same properties (upstream). Velocity profiles (Figure 2 (a), 3(a)) are extracted in various *x*-points along the channel (x_1=0.25mm, x_2=0.55mm, x_3=2.25mm, x_4=2.85mm, x_5=3.05mm), as well as in the xy-plane for $z= 4.75\times10^{-4}$ m (Figure 2 (b),3(b)). In all 3-D results the definition of the Reynolds number is based on hydraulic diameter $D_h = 4R_H = 4A/P$, where A is the cross-sectional area and P the wetted perimeter.

Both channels have identical parameters, though the inlet-outlet BCs treatment are different. We observe that in both cases velocity profiles are symmetrical and the maximum velocity is observed at the midplane as expected. There is a small difference in the mean velocity values.

The numerical solutions are in good agreement with the analytical solution in the framework of laminar creeping flow [16].

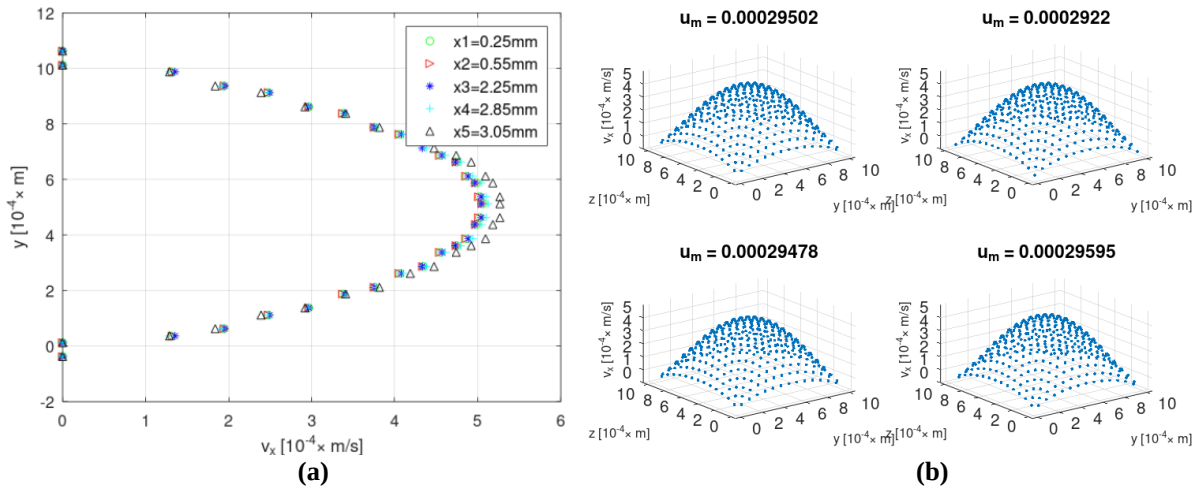

Figure 2. (a) Velocity profile for $z= 4.75\times10^{-4}$ m and 5 different x positions for a constant H1, PBCs, (b) Velocity plane and mean velocity for 4 different x position and the same channel with a constant cross-section H1 and PBCS, Re= 0.29

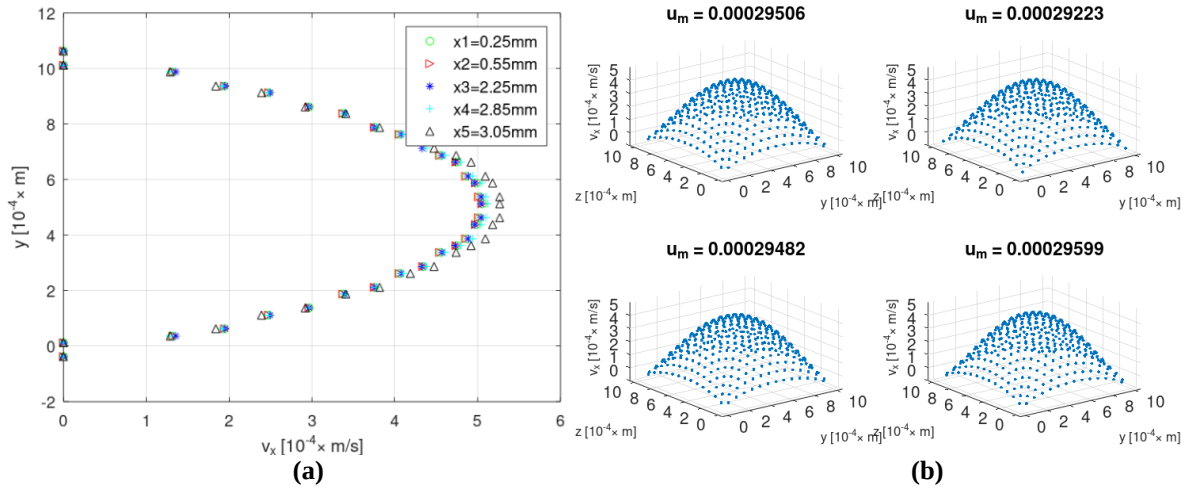

Figure 3. As in Figure 2, but with constant FBCs, Re= 0.29

4.2 Sudden expansion

Given that both PBCs and FBCs result in almost the same output in the case of a closed 3D channel with constant cross-section, a second case in which a sudden expansion occurs is investigated. A sudden 100% channel expansion with an initial H1=0.4925 mm is investigated with both FBCs and PBCs (Figures 4,5). As in previous cases mean velocity (Figure 6) and max velocity values are slightly larger at the case of FBCs.

It should be noticed that in the case of periodic boundary conditions in the flow direction, our model corresponds to a long channel with regularly repeated changes in cross-section. The simulation focuses on a single module of the channel. Furthermore the simulations become unstable and the results could be significantly diverging in case of larger Reynolds numbers [17,18,19].

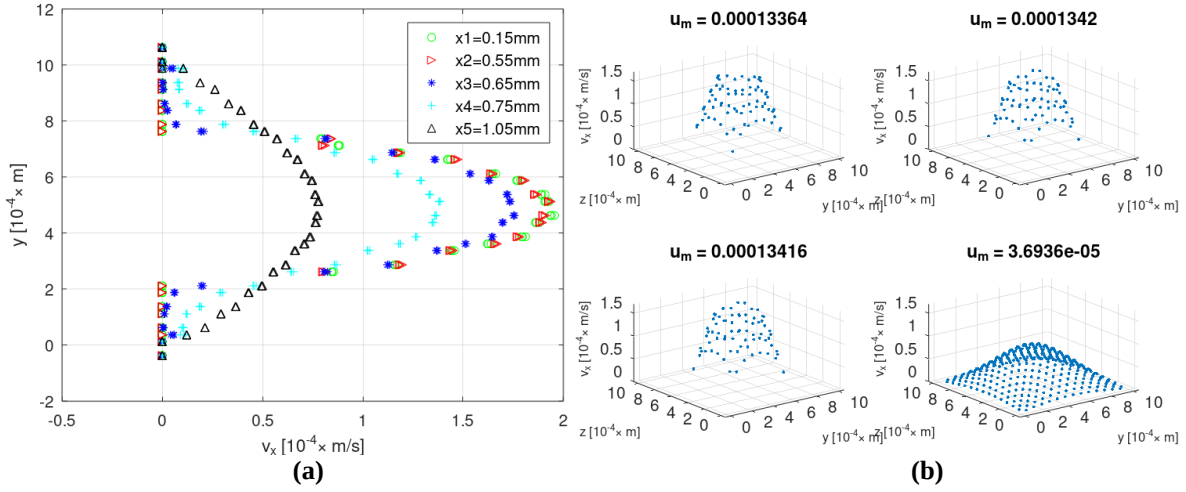

Figure 4. (a) velocity profile for z= z= 4.75×10^{-4} m and 5 different x positions for a sudden expansion 100% of a cross-section H1=0.4925 mm, FBCs, (b) Velocity plane and mean velocity for 4 different x position and the same channel for a sudden expansion 100% of a cross-section H1=0.4925 mm, FBCs, Re_s= 0.064, Re_l=0.036

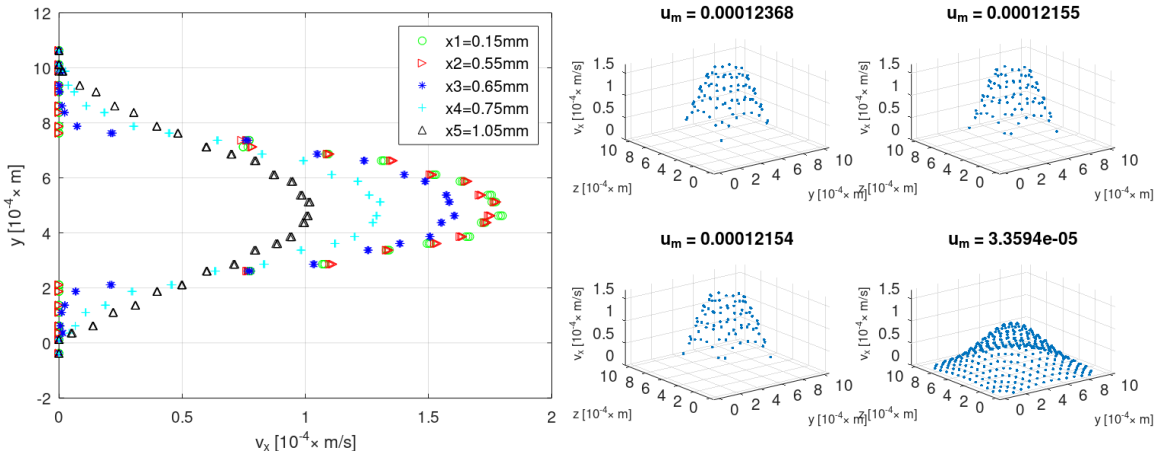

(a) **(b)**

Figure 5. (a) velocity profile for z= z= 4.75×10^{-4} m and 5 different x positions for a sudden expansion 100% of a cross-section H1=0.4925 mm, PBCs, (b) Velocity plane and mean velocity for 4 different x position and the same channel for a sudden expansion 100% of a cross-section H1=0.4925 mm, PBCs, Re_s= 0.059, Re_l= 0.033.

Table 1. Comparison between Fixed and Periodic Boundary Conditions expansion 100% H1=0.4925mm, in various channel positions.

100% Exp. Fext=1e-3				
xi	**Vi FBC (×10^{-4})**	**Vi PBC (×10^{-4})**	**Δvi (×10^{-4})**	**Relative Difference**
x1	1.34	1.24	0.10	0.07
x2	1.34	1.22	0.13	0.09
x3	0.37	0.34	0.03	0.09
x4	0.37	0.34	0.03	0.09

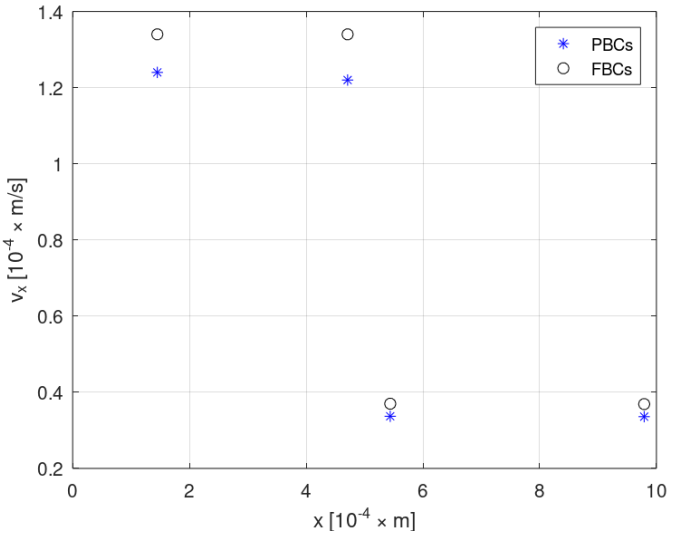

Figure 6. Mean velocity values for PBCs and FBCs.

5. NON-CREEPING LAMINAR FLOWS

In an effort to increase the Reynolds number of the flow we intend to use the DualSPHysics code. DualSPHysics solver has been initially developed for coastal engineering problems. It originates from the open-source SPHysics software and is a popular choice for carrying out simulations with millions of particles, opening the field for large real-life simulations at manageable computational time [20]. A promising modification of the Dynamic Boundary Conditions (mDBCs) has been proposed in [12], in which the "gap" between the solid wall and the fluid is reduced while the efficiency is maintened even for complex geometries.

6. CONCLUSION AND FUTURE WORK

Smoothed Particle Hydrodynamics (SPH) simulations of three dimensional flow in closed channels were carried out using the LAMMPS code with two different Boundary Conditions in the main flow direction (Periodic and Fixed). The simulation Reynolds number is very small corresponding to creeping flow regime. SPH simulations captured the main flow characteristics and the detected minor inaccuracies were observed only in the neighborhood of geometric discontinuities (corners) at the solid boundaries.

Our findings suggest that even Fixed Boundary Conditions, which means that the fluid enters the channel and leaves, has a good agreement with the Periodic Boundary simulation. In the case of constant cross-section channel, velocity profiles were almost identical. In the case of an abrupt expansion (100%) there are small or negligible differences.

Boundary conditions treatment is one of the grand challenges of SPH community. We aim to optimize boundary conditions and test more cases in different algorithmic environments applying them in micro-channels and macro-channels.

REFERENCES

[1] Groenenboom, P., Cartwright, B., McGuckin, D., Amoignon, O., Mettichi, M., Gargouri, Y., and Kamoulakos, A. Numerical studies and industrial applications of the hybrid SPH-FE method. *Comput. Fluids* (2019) **184**:40-63.

[2] Shadloo, M., Oger, G., and Le Touzé, D. Smoothed particle hydrodynamics method for fluid flows, towards industrial applications: Motivations, current state, and challenges. *Comput. Fluids* (2016) **136**:11-34.

[3] Patino-Narino, E., Idagawa, H., de Lara, D., Savu, R., Moshkalev, S., and Ferreira, L. Smoothed particle hydrodynamics simulation: a tool for accurate characterization of microfluidic devices. *J. Eng. Math.* (2019) **115**:183-205.

[4] Zhang, Z., Walayat, K., Chang, J., and Liu, M. Meshfree modeling of a fluid-particle two-phase flow with an improved SPH method. *Int. J. Numer. Methods Eng.* (2018) **116:**530-569.

[5] Monaghan, J.J. and Gingold, R.A. Shock simulation by the particle method SPH. *J. Comput. Phys.* (1983) **52**:374-389.

[6] Monaghan, J.J. Smoothed Particle Hydrodynamics. *Annu. Rev. Astron. Astrophys.* (1992) **30**:543–574.

[7] Nasar, A., Fourtakas, G., Lind, S., Rogers, B., Stansby, P., and King, J. High-order velocity and pressure wall boundary conditions in Eulerian incompressible SPH. *J. Comput. Phys.* (2021) **434**:109793.

[8] Vacondio, R., Altomare, C., De Leffe, M., Hu, X., Le Touzé, D., Lind, S. et al. Grand challenges for Smoothed Particle Hydrodynamics numerical schemes. *Comput. Part. Mech.* (2020) **8**:575-588.

[9] Perdikaris,P., Grinberg,L., and Karniadakis, G.E., Multiscale modeling and simulation of brain blood flow. *Phys. Fluids* (2016) **28**:021304.

[10] Liakopoulos A., Sofos, F., and Karakasidis, T.E. Darcy-Weisbach friction factor at the nanoscale: From atomistic calculations to continuum models. *Phys. Fluids* (2017) **29**:052003.

[11] Sofos, F., Karakasidis, T.E., and Liakopoulos, A. Fluid flow at the nanoscale: how fluid properties deviate from the bulk, *Nanosci. Nanotech. Lett.* (2013) **5**:1-4.

[12] English A., Domínguez, J.M., Vacondio, R., Crespo, A.J.C., Stansby, P.K., Lind, S.J., Chiapponi, L., Gómez-Gesteira, M. Modified dynamic boundary conditions (mDBC) for general purpose smoothed particle hydrodynamics (SPH): application to tank sloshing, dam break and fish pass problems. *Computat. Part. Mech.* (2021)

[13] Ganzenmüller, G.C., Steinhauser, M.O., Van Liedekerke, P. The implementation of Smooth Particle Hydrodynamics in LAMMPS (2011). Retrieved from http://lammps.sandia.gov/doc/PDF/SPH_LAMMPS_userguide.pdf

[14] Plimpton, S. Fast parallel algorithms for short-range molecular dynamics. *J. Comput. Phys.* (1995) **117**:1–19.

[15] Morris, J.P., Fox, P.J., Zhu, Y. Modeling low Reynolds number incompressible flows using SPH. *J. Comput. Phys.* (1997) **136**:214-226.

[16] Liakopoulos, A. *Fluid Mechanics*, Tziolas Publications (in greek) (2019) 2nd edition.

[17] Sofos, F., Chatzoglou, E., and Liakopoulos, A. An assessment of SPH simulations of sudden expansion/contraction 3-D channel flows. *Comp. Part. Mech.* (2021).

[18] Domínguez, J.M., Fourtakas, G., Altomare, C., Canelas, R.B., Tafuni, A., García-Feal, O., Martínez-Estévez, I., Mokos, A., Vacondio, R., Crespo, A.J.C., Rogers, B.D., Stansby, P.K. and Gómez-Gesteira, M. DualSPHysics: from fluid dynamics to multiphysics problems, *Comp. Part. Mech.* (2021).

[19] Liakopoulos A., Sofos F., and Karakasidis T.E. Friction factor in nanochannel flows. *Microfluid. Nanofluid.* (2016) **20**:1-7.

[20] Fourtakas, G., Rogers, B.D. Modelling multi-phase liquid-sediment scour and resuspension induced by rapid flows using Smoothed Particle Hydrodynamics (SPH) accelerated with a graphics processing unit (GPU). *Adv. Water Resour.* (2016) **92**: 186-99.